

# Coherent and incoherent atomic scattering: Formalism and application to ponium interacting with matter

T A Heim<sup>†</sup>, K Hencken<sup>†</sup>, D Trautmann<sup>†</sup> and G Baur<sup>‡</sup>

<sup>†</sup> Institut für Theoretische Physik, Universität Basel, 4056 Basel, Switzerland

<sup>‡</sup> Institut für Kernphysik, Forschungszentrum Jülich, 52425 Jülich, Germany

**Abstract.** The experimental determination of the lifetime of ponium provides a very important test on chiral perturbation theory. This quantity is determined in the DIRAC experiment at CERN. In the analysis of this experiment, the breakup probabilities of ponium in matter are needed to high accuracy as a theoretical input. We study in detail the influence of the target electrons. They contribute through screening and incoherent effects. We use Dirac-Hartree-Fock-Slater wavefunctions in order to determine the corresponding form factors. We find that the inner-shell electrons contribute less than the weakly bound outer electrons. Furthermore, we establish a more rigorous estimate for the magnitude of the contribution from the transverse current (magnetic terms thus far neglected in the calculations).

PACS numbers: 36.10.-k, 34.50.-s, 13.40.-f

## 1. Introduction

In experiments such as atom-atom scattering, atom-electron scattering, nuclear scattering at high energy, or photo-production of  $e^+e^-$  pairs on atoms one faces the situation of complex systems undergoing transitions between different internal states. For an atomic target, excitation affects the electrons individually. Thus the “form factor” for the target-inelastic process takes the form of an *incoherent* sum over all electrons, as opposed to the *coherent* action of the electrons (and the nucleus) in the target-elastic case. From this observation it is immediately obvious that the target-inelastic cross section is proportional to  $Z$ , the number of electrons in the target atom, whereas the target-elastic process scales with  $Z^2$ . Since incoherent scattering off the excited target electrons increases the cross section from its value due to coherent scattering off the atom, the effect is sometimes referred to as “anti-screening” [1, 2]. At large momentum transfer the anti-screening correction can be accurately approximated by increasing the coherent scattering cross section by the factor  $(1 + 1/Z)$ , see e.g. [3, 4, 5]. We will demonstrate in this article, however, that this simple re-scaling argument is not sufficiently accurate in general. At the same time we will show how to obtain far superior results in a Dirac-Hartree-Fock-Slater approach with manageable numerical effort.

As an application of the general formalism discussed in this paper, we put our focus on the particular situation pertaining to experiment DIRAC. This experiment, currently being performed at CERN [6], aims at measuring the lifetime of ponium,

i.e., a  $\pi^+\pi^-$  pair forming a bound state as an exotic, hydrogen-like atom. While moving through matter, this system can breakup via electromagnetic interaction, or it can annihilate in the strong hadronic decay  $\pi^+\pi^- \rightarrow \pi^0\pi^0$  if the ponium is in an  $s$ -state. The lifetime for this decay is related to the  $\pi\pi$  scattering length which in turn has been calculated in the framework of chiral perturbation theory. Experiment DIRAC therefore provides a crucial test for a theoretical low-energy QCD prediction of pion–pion scattering. The ponium is formed from pions produced in the collision of a high energy proton beam on a (heavy element) target foil on condition that the two charged pions have small relative momentum. The ponium production rate can be inferred from the double inclusive production cross section for  $\pi^+\pi^-$ -pairs without final state Coulomb interaction. The kinematical conditions of the experiment (target thickness of 100 to 200  $\mu\text{m}$ , compared to a predicted decay length in the lab of roughly 15 to 20  $\mu\text{m}$ ) imply annihilation of the ponium through strong interaction still within the target foil. However, the experiment does not measure the neutral pions. Instead, *charged* pions are actually detected, and pions from electromagnetic breakup of “atomic” pairs are distinguished by small relative momentum and small angular separation from a large background of accidental “free” pairs with arbitrary momentum and no directional correlation. Comparing the observed “ionized” atomic pairs with the number of ponium atoms produced for a given target material and thickness, one can extract the lifetime for the hadronic decay. Thus very accurate cross sections for the electromagnetic interaction between ponium and the target material are needed as an input in the analysis of the experiment.

The paper is organized as follows: In section 2 we review the well established formalism for one-photon exchange, applied e.g. in electron–hadron scattering. In section 3 the cross sections coming from the transverse photons are estimated with the help of the long-wavelength limit. The formulas for the evaluation of atomic form factors and scattering functions in the framework of Dirac-Hartree-Fock-Slater theory are derived in section 4, followed by an analysis of simple alternative models in section 5. Although the results presented in section 6 have been obtained in the context of experiment DIRAC, many of the conclusions drawn in section 7 are also valid more generally in atomic scattering.

## 2. Formalism

In [7] we applied the semiclassical approximation to calculate the coherent (target-elastic) cross section for ponium–atom scattering, demonstrating that this part can indeed be determined with the desired accuracy of 1%. However, contributions not yet included in [7] need to be added to achieve an overall accuracy at the 1% level. Here we are interested in those processes, where the atom is excited together with the ponium. We will treat the problem within the PWBA. For our derivation we will follow closely the standard formalism of electron scattering as found, e.g., in [8, 9, 10].

We only calculate the lowest order result. The relevant Feynman diagram is shown in figure 1. The cross section for this process is given by

$$\sigma = \frac{1}{4I} \frac{1}{(2\pi)^2} 2M_A 2M_\Pi \int d^4q \frac{(4\pi e^2)^2 W_A^{\mu\nu} W_{\mu\nu\Pi}}{(q^2)^2}, \quad (1)$$

where  $I$  is the incoming flux, and  $W_A^{\mu\nu}$  and  $W_\Pi^{\mu\nu}$  are the electromagnetic tensors describing the electromagnetic interaction of atom and ponium with the photon. As we are not interested in the specific final state of the atom, we can average over the

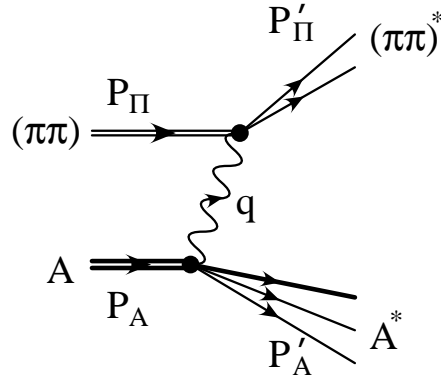


**Figure 1.** The lowest order Feynman diagram for the simultaneous excitation of projectile (pionium) and target (atom). The atomic momenta are  $P_A$  and  $P'_A$  before and after the collision, those of the pionium  $P_\Pi$  and  $P'_\Pi$ . The momentum of the exchanged photon is  $q = P'_\Pi - P_\Pi = -(P'_A - P_A)$ .

possible initial spin and sum over all final states and directions corresponding to a specific final state momentum  $P'$ . For the atom we have

$$W_A^{\mu\nu} = \frac{1}{4\pi M_A} \sum_X \langle 0, P_A | J^{\mu\dagger} | X, P'_A \rangle \langle X, P'_A | J^\nu | 0, P_A \rangle (2\pi)^4 \delta^4(P_A - q - P'_A) \quad (2)$$

and similarly for the pionium if its final state is not resolved either.

The electromagnetic tensor can only be a function of  $P$  and  $P'$ , or equivalently, of  $P$  and  $q$ . Gauge invariance or current conservation restricts the possible tensor structure of  $W^{\mu\nu}$  even more. It is a well known result that the electromagnetic tensor in this case only depends on two scalar functions  $W_1$  and  $W_2$  that are functions of  $q^2$  and  $Pq$  alone. The electromagnetic tensor is then given by

$$W^{\mu\nu} = \left( -g^{\mu\nu} + \frac{q^\mu q^\nu}{q^2} \right) W_1(q^2, Pq) + \left( P^\mu - \frac{Pq q^\mu}{q^2} \right) \left( P^\nu - \frac{Pq q^\nu}{q^2} \right) \frac{W_2(q^2, Pq)}{M^2}. \quad (3)$$

Since the cross section depends on the product of the tensor for the atom and the pionium, we calculate this product in terms of  $W_1$  and  $W_2$ :

$$W_A^{\mu\nu} W_{\mu\nu\Pi} = 3W_{1,\Pi} W_{1,A} + \left( -1 + \frac{\Delta^2}{q^2} \right) W_{1,\Pi} W_{2,A} + \left( -1 + \frac{\omega^2}{q^2} \right) W_{2,\Pi} W_{1,A} + \left( \gamma + \frac{\omega\Delta}{q^2} \right)^2 W_{2,\Pi} W_{2,A}, \quad (4)$$

where  $\gamma$  is the (relative) Lorentz factor between atom and pionium,  $\Delta = -P_A q / M_A$ ,  $\omega = P_\Pi q / M_\Pi$  are (minus) the energy of the exchanged photon in the atom and pionium rest frame, respectively. Following the argument of [11, 7] we expect the cross section to be dominated by the charge operator (termed “scalar interaction” in [7]). Thus we neglect at this point all terms containing a  $W_1$ . We note also that  $W_1$  vanishes in the elastic case for spin 0 particles. However, the contribution to the cross section coming from  $W_1$  will be discussed in section 3 below in the analysis of the transverse part of the current operator  $\mathbf{j}$ . Keeping only the last term and assuming that the pre-factor is dominated by  $\gamma$  ( $\gamma$  is in the range 15–20 in the DIRAC experiment) we get

$$W_A^{\mu\nu} W_{\mu\nu\Pi} \approx \gamma^2 W_{2,\Pi} W_{2,A}. \quad (5)$$

Although this coincides with the naive estimate obtained by superficially identifying the leading power of  $\gamma$  (assumed to be dominant), one should keep in mind that (as will be shown below) the range of  $q^2$  starts at about  $(\omega/\gamma)^2$  or  $(\Delta/\gamma)^2$ , where the last three pre-factors are of the same order. The magnitude of  $\gamma$  should therefore not be mistaken as a justification for neglecting the terms containing  $W_1$ . A critical assessment of the relative importance of  $W_1$  as compared to  $W_2$  is postponed until section 3.

In our application to ponium–atom scattering the masses  $M_A$  and  $M_\Pi$  will be much larger than the momentum transfer  $q$  of the photon. Therefore we will neglect recoil effects on the atom and ponium. We can then identify  $\Delta$  and  $\omega$  as the excitation energy of the atom and ponium in their respective rest frames. Therefore  $q_0$  and  $q_z$  are fixed by the values of  $\omega$  and  $\Delta$ . In the following we will always denote the spatial part of the photon momentum in the rest frame of the atom by  $\mathbf{k}$  and in the rest frame of the ponium by  $\mathbf{s}$ . In the rest frame of the atom we then have

$$\begin{aligned} q_{0,A} &= -\Delta \\ q_{z,A} = k_z &= -\frac{\Delta}{\beta} - \frac{\omega}{\gamma\beta}, \end{aligned} \quad (6)$$

and in the rest frame of the ponium

$$\begin{aligned} q_{0,\Pi} &= \omega \\ q_{z,\Pi} = s_z &= -\frac{\Delta}{\gamma\beta} - \frac{\omega}{\beta}. \end{aligned} \quad (7)$$

Also  $q^2$  is given by

$$q^2 = -\left(\frac{\Delta^2}{\beta^2\gamma^2} + \frac{\omega^2}{\beta^2\gamma^2} + \frac{2\omega\Delta}{\beta^2\gamma} + q_\perp^2\right) =: -(q_i^2 + q_\perp^2). \quad (8)$$

Replacing the integration over  $d^4q = \frac{1}{\gamma\beta} d\omega d\Delta d^2q_\perp$ , we obtain

$$\sigma = \int d\omega d\Delta d^2q_\perp \frac{4\alpha^2}{\beta^2} \frac{W_{2,\Pi}(\omega, q^2) W_{2,A}(\Delta, q^2)}{(q_i^2 + q_\perp^2)^2}. \quad (9)$$

From (8) we note that  $q_i^2$  may become negative if for example the ponium is initially in an excited state and gets de-excited ( $\omega < 0$ ) while the target atom gets excited ( $\Delta > 0$ ) from its ground state. For this process the cross section (9) has a formal singularity, as pointed out recently in [12]. Formally the divergence arises from integrating over the impact parameter all the way to infinity. Under the conditions of the experiment DIRAC, however, this formal divergence is negligible compared to the principal value of the cross section integral.

One of the advantages of this derivation is that the  $W_2$  are scalar functions; we can therefore evaluate them in the respective rest frames, even though the relative motion of atom and ponium is relativistic. We now establish a relation between  $W_2$  and the electromagnetic transition currents. As was already done in [7] we assume the charge operator to be the dominant contribution. In the atom's rest frame  $W_2$  is related to the '00'-component of the tensor through

$$W_{2,A} = \frac{q^4}{k^4} W_{\text{rf},A}^{00}, \quad (10)$$

see, e.g., [13, 14], with  $k^2 = \mathbf{k}^2 = \Delta^2 - q^2$ . Here we have added an index ‘‘rf’’ as a reminder that the ‘00’-component in the rest frame has to be taken. From the definition of  $W^{\mu\nu}$  we get

$$W_A^{00} = \frac{1}{4\pi M_A} \sum_X \langle 0 | J^{0\dagger}(q) | X, P'_A \rangle \langle X, P'_A | J^0(q) | 0 \rangle (2\pi)^4 \delta^4(P_A - q - P'_A). \quad (11)$$

Rewriting this expression in terms of the (non-relativistic) density operator and again neglecting recoil effects we find

$$W_A^{00} = \sum_X \langle 0 | \rho(\mathbf{q}) | X, E_X \rangle \langle X, E_X | \rho(\mathbf{q}) | 0 \rangle \delta(E_{0,A} + \Delta - E_X) \quad (12)$$

$$= \sum_X |F_{X0,A}(\mathbf{q})|^2 \delta(E_{0,A} + \Delta - E_X). \quad (13)$$

(Replacing the energy  $E$  by the rest mass  $M$  in these weakly bound systems only introduces an error of the order  $\alpha^2$ ). Finally we obtain for the cross section:

$$\sigma = \int d\omega d\Delta d^2q_\perp \frac{4\alpha^2}{\beta^2} \frac{q^4}{s^4 k^4} \left[ \sum_X |F_{X0,A}(\mathbf{k})|^2 \delta(E_{0,A} + \Delta - E_X) \right] \times \left[ \sum_{X'} |F_{X'0,\Pi}(\mathbf{s})|^2 \delta(E_{0,\Pi} + \omega - E_{X'}) \right]. \quad (14)$$

As a verification of this formalism we reproduce the result of [7] for target-elastic scattering. In this case  $\Delta = 0$  and  $k^2 = q^2$ , and the only possible final state is  $X = 0$  (assuming no degeneracy of the ground state). We find

$$\sigma = \int d\omega d^2q_\perp \frac{4\alpha^2}{\beta^2} \frac{1}{s^4} |F_{00,A}(\mathbf{q})|^2 \left[ \sum_X |F_{X0,\Pi}(\mathbf{s})|^2 \delta(E_{0,\Pi} + \omega - E_X) \right], \quad (15)$$

and  $F_{00,A}(\mathbf{q})$  is the elastic form factor of the atom. This is identical to the equation derived in [7] in the Coulomb gauge ( $\mathbf{k} \cdot \mathbf{A} = 0$ ).

At this point we should add a few comments regarding the gauge invariance and the factor  $q^4/k^4$  (and likewise  $q^4/s^4$ ) in (10): In determining the general tensor structure of  $W^{\mu\nu}$  in (3) the gauge invariance (or alternatively current conservation) was used. The magnitude of the component of  $\mathbf{j}$  along the direction of  $\mathbf{q}$  is then fixed by  $\rho$ . Only the transverse parts of the current remain independent quantities. Our result therefore agrees with the one in Coulomb gauge, as in this gauge the component of  $\mathbf{A}$  along the direction of  $\mathbf{q}$  vanishes. An alternative approach might start directly from  $W^{\mu\nu}$  without decomposition into  $W_1$  and  $W_2$ . Assuming that in the rest frame of either the atom or the pionium  $W^{00}$  dominates, one can approximate the product of the electromagnetic tensors by

$$W_A^{\mu\nu} W_{\mu\nu\Pi} \approx \gamma^2 W_{\text{rf},A}^{00} W_{\text{rf},\Pi}^{00} \quad (16)$$

where the factor  $\gamma^2$  comes from the Lorentz transformation of one tensor into the rest frame of the other. Now using (16) instead of (10), the cross section reads

$$\sigma = \int d\omega d\Delta d^2q_\perp \frac{4\alpha^2}{\beta^2} \frac{1}{q^4} \left[ \sum_X |F_{X0,A}(\mathbf{k})|^2 \delta(E_{0,A} + \Delta - E_X) \right] \times \left[ \sum_{X'} |F_{X'0,\Pi}(\mathbf{s})|^2 \delta(E_{0,\Pi} + \omega - E_{X'}) \right]. \quad (17)$$

This differs from (14) by a factor  $q^4/k^4 \cdot q^4/s^4$ . In the elastic case (17) corresponds to the result of [7] in the Lorentz gauge. However, the approximation (16) and therefore also (17) is not gauge invariant, whereas (14) is by construction. We will therefore prefer in the following the form as given in (14). In [7] the difference between the two results was interpreted as an indicator for the magnitude of the “magnetic terms”, that is, the contribution proportional to  $\mathbf{j}$ . In the next section we will estimate the contribution of the transverse photons, making use of the long-wavelength limit. It remains to be seen, however, which one of the two possible schemes (longitudinal/transverse decomposition versus scalar/magnetic terms) will be better suited for explicit calculations.

In order to determine total cross sections we would like to simplify the summation over all possible states. The expression (14) depends on  $\omega$  and  $\Delta$  in two ways: Through the energy-conserving delta functions and through the expression for  $q^2$ , where  $q_l^2 = \Delta^2/(\beta^2\gamma^2) + \omega^2/(\beta^2\gamma^2) + (2\omega\Delta)/(\beta^2\gamma)$  depends on both  $\omega$  and  $\Delta$ . Replacing  $\omega$  and  $\Delta$  in  $q_l$  by some average values  $\omega_0$  and  $\Delta_0$ , we can perform the closure over all final states to get

$$\sigma = \int d^2q_{\perp} \frac{4\alpha^2}{\beta^2} \frac{q^4}{s^4 k^4} S_{\text{inc,A}}(\mathbf{k}) S_{\text{inc,\Pi}}(\mathbf{s}) \quad (18)$$

with  $q^2, s^2$ , and  $k^2$  now the ones using  $\omega_0$  and  $\Delta_0$  and

$$S_{\text{inc,A}}(\mathbf{k}) = \sum_X |F_{X0,A}(\mathbf{k})|^2 \quad (19)$$

$$S_{\text{inc,\Pi}}(\mathbf{s}) = \sum_{X'} |F_{X'0,\Pi}(\mathbf{s})|^2. \quad (20)$$

In section 6 the dependence of the cross section on the choice of  $\Delta_0$  and  $\omega_0$  will be studied by varying both parameters over a reasonable range. For the atomic scattering function  $S_{\text{inc,A}}$ , this study requires analyzing the contributions of individual electron excitations shell by shell, since the binding energies vary from some eV to several keV for the different shells.

### 3. Contribution of transverse photons

In section 2 we have only calculated the effect coming from the longitudinal photons (that is, coming from the charge operator). Already in [11, 7] the effect of the so-called “magnetic interaction”, that is, the effect of the current operator was estimated to be of the order of 1%. As the DIRAC experiment requires an accuracy of 1%, these contributions need to be considered more carefully. The part of the current operator  $\mathbf{j}$  in the direction of  $\mathbf{q}$  is already included in the above calculation. Therefore we need to study only the contribution coming from the transverse part of the current operator, that is, the effect coming from the transverse photons. Here we estimate them with the help of the long-wavelength approximation. Following [13], see also [14],  $W_1$  and  $W_2$  can be expressed in terms of the Coulomb and transverse electric (magnetic) matrix elements:

$$W_1 = 2\pi (|T^e|^2 + |T^m|^2) \quad (21)$$

$$W_2 = \frac{q^4}{s^4} 2\pi \left( 2|M^C|^2 - \frac{s^2}{q^2} (|T^e|^2 + |T^m|^2) \right), \quad (22)$$

where we use the usual definitions for  $M^C$  and  $T^{e,m}$ :  $W^{00} = 4\pi|M^C|^2$  and  $W^{\lambda\lambda'} = \delta^{\lambda\lambda'} 2\pi (|T^e|^2 + |T^m|^2)$  with  $\lambda, \lambda'$  denoting the two transverse directions. The  $T^m$  can

be safely neglected in our case. The long-wavelength limit relates  $T^e$  to  $M^C$ . In the multipole expansions

$$T^e = \sum_{J \geq 1} \sum_M T_{JM}^e, \quad M^C = \sum_{J \geq 0} \sum_M M_{JM}^C, \quad (23)$$

we have for a given multipole [8, 15]

$$T_{JM}^e \approx \frac{\omega}{s} \left( \frac{J+1}{J} \right)^{1/2} M_{JM}^C, \quad \text{for } J \geq 1. \quad (24)$$

In the case of the pionium only odd multipoles contribute and there is thus no  $M_{00}^C$  term. As higher multipoles are strongly suppressed we can safely set the factor  $(J+1)/J$  to its maximum value at 2 (i.e.  $J=1$ ) for the purpose of an analytical estimate for the upper limit of  $|T^e|$ . However, since our computer program already contains a multipole expansion, it is of course straightforward to perform a more refined numerical calculation. For the atom, on the other hand,  $M_{00}^C \neq 0$ ; it is in fact the dominant contribution in the elastic process. Although generalizing the relation (24) with the maximum factor  $\sqrt{2}$  for all multipole orders still provides an upper limit for  $T^e$ , it may be a less useful over-estimate for the atom. The relation between  $|M^C|^2$  and  $|T^e|^2$  is then approximately

$$|T^e(q)|^2 \approx 2 \frac{\omega^2}{s^2} |M^C(q)|^2 \quad (25)$$

$$\approx \frac{1}{2\pi} \frac{\omega^2}{s^2} W_{\text{rf}}^{00}. \quad (26)$$

One sees that the transverse photons contribute to both  $W_1$  and  $W_2$ . Denoting their contribution by  $W_1^T$  and  $W_2^T$ , they can be expressed with the help of (21), (22), and (26) as

$$W_1^T = \frac{\omega^2}{s^2} W_{\text{rf}}^{00}, \quad (27)$$

$$W_2^T = \frac{-q^2 \omega^2}{s^4} W_{\text{rf}}^{00}. \quad (28)$$

First we look at the elastic case (for the atom). In this case we have  $\Delta = 0$ ,  $W_{1,A} = 0$  and  $W_{\text{rf},A}^{00} = |F_{00,A}(\mathbf{q})|^2$ . The product of the electromagnetic tensors is then

$$W_A^{\mu\nu} W_{\mu\nu\Pi} = -W_{1,\Pi}^T W_{2,A} + \gamma^2 W_{2,\Pi}^T W_{2,A} \quad (29)$$

$$= \frac{\omega^2}{s^2} \left( -1 + \gamma^2 \frac{-q^2}{s^2} \right) W_{\text{rf},\Pi}^{00} |F_{00,A}(\mathbf{q})|^2. \quad (30)$$

Again summing over all excited states of the pionium and neglecting the dependence on  $\omega$  in  $q^2$  and  $s^2$  we get the total cross section

$$\sigma_{\text{el}}^T = \int d^2 q_{\perp} \frac{4\alpha^2 \omega^2}{\beta^2 s^2} \left( -\frac{1}{\gamma^2 q^4} + \frac{1}{s^2(-q^2)} \right) S_{\text{inc},\Pi}(\mathbf{s}) |F_{00,A}(\mathbf{q})|^2. \quad (31)$$

We see that this cross section differs from (15) by the replacement

$$\frac{1}{s^4} \rightarrow \frac{\omega^2}{s^2} \left( -\frac{1}{\gamma^2 q^4} + \frac{1}{s^2(-q^2)} \right) \quad (32)$$

The estimate for the reduction of these terms compared to the charge contribution can be seen easily in this equation, if one assumes that the dominant contributions come from the range of  $q^2$  (and therefore also of  $s^2$ ) of the order of  $k_{\Pi}^2$ , where  $k_{\Pi}$

denotes the Bohr-momentum of the pionium,  $k_{\Pi} = 1/a_{\text{Bohr},\Pi} \approx 136.566/a_{\text{Bohr}}$ . This momentum is of the order  $\omega/\alpha$ . Therefore the factor  $\omega^2/s^2$  would give a reduction of the order  $\alpha^2$ , making this contribution completely negligible. However, a discussion of the relevant range of  $q^2$  to be given in section 6 will show that this estimate is too crude.

In the inelastic case (on the atom side) we can approximately set  $\Delta_0 \approx 0$  again, as the atomic binding energy is small compared to the other energies. Then the contribution from the transverse current of the atom will be suppressed even more than for the pionium, since the ratio  $\Delta/k$  is even smaller than  $\omega/s$ . The only difference compared to (31) is then the replacement of  $|F_{00,A}(\mathbf{q})|^2$  by  $S_{\text{inc},A}(\mathbf{k})$ . We get

$$\sigma_{\text{inel}}^{\text{T}} = \int d^2q_{\perp} \frac{4\alpha^2 \omega^2}{\beta^2 s^2} \left( -\frac{1}{\gamma^2 q^4} + \frac{1}{s^2(-q^2)} \right) S_{\text{inc},\Pi}(\mathbf{s}) S_{\text{inc},A}(\mathbf{k}). \quad (33)$$

We will discuss the contribution to the cross section in section 6.

#### 4. Dirac-Hartree-Fock-Slater model

We now turn to the question how to evaluate the form factors and scattering functions derived in the general formalism of the preceding sections. For our specific application of pionium scattering off atomic targets, we use the pionium form factors as described in [7]; here we shall only discuss the calculation of the *atomic* form factors.

The purpose of this explicit calculation of atomic form factors and especially atomic scattering functions is twofold: Existing tables [16] give no indication about the contributions from individual atomic shells, an information that is crucially needed to determine the appropriate average excitation energy in the closure approximation. Furthermore, since target atoms as heavy as Pt ( $Z = 78$ ) will be employed in the experiment DIRAC, the atomic structure is more appropriately treated with relativistic orbitals, at variance with the non-relativistic calculations in [16].

##### 4.1. Atomic ground state elastic form factors

Within the framework of (Dirac-)Hartree-Fock-Slater theory, the atomic ground state wavefunction entering the expression for the form factor,

$$F_{00}(\mathbf{k}) = \langle \Psi_0 | \sum_{j=1}^Z \exp(i\mathbf{k} \cdot \mathbf{r}_j) | \Psi_0 \rangle, \quad (34)$$

is given by a single Slater determinant constructed from products of independent particle orbitals,

$$\Psi_0 = \frac{1}{\sqrt{Z!}} \sum_p \text{sign}(p) \Phi_{p(1)}(\mathbf{r}_1) \cdots \Phi_{p(Z)}(\mathbf{r}_Z). \quad (35)$$

Here  $Z$  denotes the nuclear charge (and the number of electrons), while  $p$  denotes the permutations of orbital indices, and  $\Phi_j$  signify single particle orbitals. Each of the  $Z$  exponential terms  $\exp(i\mathbf{k} \cdot \mathbf{r}_j)$  in (34) acts as a one-particle operator. Orthogonality of the orbitals effectively cancels the summation over permutations in the bra and ket vectors leading to

$$F_{00}(\mathbf{k}) = \sum_{j=1}^Z \langle \Phi_j(\mathbf{r}_j) | \exp(i\mathbf{k} \cdot \mathbf{r}_j) | \Phi_j(\mathbf{r}_j) \rangle. \quad (36)$$



So far we have not considered any angular momentum coupling of the independent-particle orbitals, that is, our  $\Psi_0$  is determined by a set of quantum numbers  $(n_j, l_j, m_j)$ ,  $j = 1 \dots Z$ , without coupling to a total  $L$  (or  $J$ ) and  $M$ . Furthermore we assumed the ground state wavefunction in the bra and ket symbols to be identical. This need not actually be the case, as different  $z$ -projections  $M$  of the total angular momentum  $J$  of the ground state cannot be distinguished (without external fields). The angular momentum coupled ground state wavefunction would then be obtained by summing and averaging over  $M$  and  $M'$  in the bra and ket vectors, respectively. Likewise on the level of independent particle labels  $m_j$ , the orthogonality argument applies strictly only to all orbitals except  $j$ , that is, we should distinguish between  $m_j$  and  $m'_j$  for the bra and for the ket vector, respectively. Since the one-particle operator does not affect the spin part of the wavefunction, we should also insert an orthogonality factor for the spin orbitals in bra and ket,  $\chi_j, \chi'_j$ . Of course the principal and azimuthal quantum number  $n_j$  and  $l_j$  coincide in the bra and in the ket symbol.

Expanding the exponential in spherical harmonics we find immediately

$$F_{00}(\mathbf{k}) = \sum_{j=1}^Z (2l_j + 1) \delta_{\chi_j, \chi'_j} \sum_{\lambda, \mu} i^\lambda \sqrt{4\pi} Y_{\lambda, \mu}^*(\hat{k}) \sqrt{2\lambda + 1} \begin{pmatrix} l_j & l_j & \lambda \\ 0 & 0 & 0 \end{pmatrix} \times \\ (-1)^{m'_j} \begin{pmatrix} l_j & l_j & \lambda \\ m_j & -m'_j & \mu \end{pmatrix} \mathcal{R}_{jj}^\lambda(k), \quad (37)$$

with the radial form factor defined by

$$\mathcal{R}_{ij}^\lambda(k) = \int_0^\infty dr r^2 R_{n_i l_i}(r) j_\lambda(kr) R_{n_j l_j}(r), \quad (38)$$

where the  $R_{nl}(r)$  denote radial wavefunctions for the orbitals, and  $j_\lambda(kr)$  is a spherical Bessel function.

In a next step averaging  $|F_{00}(\mathbf{k})|^2$  over all directions  $\hat{q}$  and using the orthogonality relation of the spherical harmonics yields

$$|F_{00}(k)|^2 := \frac{1}{4\pi} \int d\hat{k} |F_{00}(\mathbf{k})|^2 \\ = \sum_{\lambda, \mu} (2\lambda + 1) \left\{ \sum_{j=1}^Z (-1)^{m'_j} (2l_j + 1) \delta_{\chi_j, \chi'_j} \begin{pmatrix} l_j & l_j & \lambda \\ 0 & 0 & 0 \end{pmatrix} \times \right. \\ \left. \begin{pmatrix} l_j & l_j & \lambda \\ m_j & -m'_j & \mu \end{pmatrix} \mathcal{R}_{jj}^\lambda(k) \right\}^2. \quad (39)$$

Obviously all electrons contribute coherently to the form factor, as expected. Due to the first  $3j$ -symbol only even multipoles contribute to the sum.

In the  $LS$ -coupling scheme, the atomic ground state is characterized by a specific total  $L$  and a (possibly averaged) total  $M$ . Instead of coupling the individual electrons' angular momenta to total  $L$  and then averaging over  $M$ , we average directly over individual  $m_j, m'_j$  for the orbitals occupied in accordance with the Pauli principle. This amounts to neglecting energy differences between fine structure levels. Hund's rules (see e.g. [17]) state that sub-shells are to be filled by adding as many electrons with different  $m_j$  and the same spin projection as possible. The critical multiplicity is thus that for a half filled sub-shell,  $(2l + 1)$ . For half filled or completely filled sub-shells, Hund's rules imply that both  $m_j$  and  $m'_j$  run over all possible values from  $-l_j$  to

$+l_j$ . Consequently the angular part for these spherical sub-shells reduces to selecting only monopole contributions. A completely filled sub-shell  $(n_j, l_j)$  thus contributes

$$2(2l_j + 1)\mathcal{R}_{jj}^0(k)$$

to the full form factor. (The leading factor 2 indicates the spin multiplicity.)

For sub-shells that are neither completely nor half filled the averaging procedure yields different multiplicities depending on the multipole order. For the dominating monopole contribution, this factor is simply given by the occupation number of the sub-shell, whereas for higher multipoles this factor is proportional to the product of occupation number and the number of holes in a sub-shell with identical spin projections. For a given number of electrons in an open sub-shell we averaged the  $m$ -dependent part in (39) over all possible distributions of  $m_j$  and  $m'_j$  values.

Note that the coherent (elastic) form factor  $F_{00}(k)$  derived above describes only the effect of scattering off the atomic electrons. The complete elastic form factor for the atom reads

$$F_{\text{Atom}}(k) = Z - F_{00}(k), \quad (40)$$

assuming a point-like nucleus.

#### 4.2. Atomic inelastic scattering functions

Besides the elastic form factor  $F_{00}(\mathbf{k})$  treated in the preceding section, we also need to consider the contributions due to excitations of the atomic electron cloud. Nuclear excitations will not be considered here because the much larger excitation energy required (typically on the order of MeV) exceeds the energy range relevant for our application to pionium-atom scattering. We demonstrated in [7] that deviations from a point-like nucleus are negligible for the electromagnetic processes considered here. Thus the nucleus' internal structure with its excited states is equally irrelevant as the experiment DIRAC cannot probe this structure. In analogy to the elastic form factor, a transition form factor is written in the form

$$F_{X0}(\mathbf{k}) = \langle \Psi_X | \sum_{j=1}^Z \exp(i\mathbf{k} \cdot \mathbf{r}_j) | \Psi_0 \rangle, \quad (41)$$

corresponding to scattering with excitation of the atomic electrons from the ground state to some excited state  $X$ . A similar expression was studied in [18] in the context of the equivalent photon approximation. The total inelastic scattering function is defined as the incoherent sum over all states  $X$  other than the ground state

$$\begin{aligned} S_{\text{inc}}(\mathbf{k}) &= \sum_{X \neq 0} |F_{X0}(\mathbf{k})|^2 \\ &= \sum_{\text{all } X} |F_{X0}(\mathbf{k})|^2 - |F_{00}(\mathbf{k})|^2 \\ &= Z + \sum_{i=1}^Z \sum_{j \neq i}^Z \langle \Psi_0 | \exp(i\mathbf{k} \cdot [\mathbf{r}_j - \mathbf{r}_i]) | \Psi_0 \rangle - |F_{00}(\mathbf{k})|^2. \end{aligned} \quad (42)$$

Here we have added the ground state in order to exploit the completeness of the set of states  $\{X\}$ : Expanding the squared modulus of  $F_{X0}$  introduced a second (primed) set of variables  $\mathbf{r}'_j$  which has been removed again by virtue of the completeness of the set of states  $\{X\}$ . Furthermore we evaluated the sum over the diagonal terms  $i = j$

separately, obtaining the term  $Z$  (since  $\exp(i\mathbf{k} \cdot [\mathbf{r}_j - \mathbf{r}_i]) \equiv 1$  in this case). Using the same Slater determinant wavefunctions for  $\Psi_0$  as in the preceding section, expanding the double sum corresponding to  $|F_{00}(\mathbf{k})|^2$ , and combining terms with the last sum, we find (in terms of the single-electron orbitals)

$$S_{\text{inc}}(\mathbf{k}) = Z - \sum_{i=1}^Z \sum_{j=1}^Z |\langle \Phi_i | \exp(i\mathbf{k} \cdot \mathbf{r}) | \Phi_j \rangle|^2. \quad (43)$$

The new terms required in the determination of  $S_{\text{inc}}$  are the matrix elements

$$\begin{aligned} \langle \Phi_i | \exp(i\mathbf{k} \cdot \mathbf{r}) | \Phi_j \rangle &= \delta_{\chi_i \chi_j} (-1)^{m_i} \sqrt{4\pi(2l_i + 1)(2l_j + 1)} \sum_{\lambda, \mu} Y_{\lambda, \mu}^*(\hat{k}) i^\lambda \sqrt{2\lambda + 1} \times \\ &\quad \begin{pmatrix} l_i & l_j & \lambda \\ 0 & 0 & 0 \end{pmatrix} \begin{pmatrix} l_i & l_j & \lambda \\ -m_i & m_j & \mu \end{pmatrix} \mathcal{R}_{ij}^\lambda(k), \end{aligned} \quad (44)$$

some of which (namely, those with  $i = j$ ) have already been used in calculating  $F_{00}(\mathbf{k})$ . As before,  $\chi_i, \chi_j$  denote the spin projections. Averaging over the directions  $\hat{k}$  we obtain immediately

$$\begin{aligned} S_{\text{inc}}(k) &:= \frac{1}{4\pi} \int d\hat{k} S_{\text{inc}}(\mathbf{k}) \\ &= Z - \sum_{i=1}^Z \sum_{j=1}^Z \delta_{\chi_i \chi_j} (2l_i + 1)(2l_j + 1) \sum_{\lambda} (2\lambda + 1) \begin{pmatrix} l_i & l_j & \lambda \\ 0 & 0 & 0 \end{pmatrix}^2 \times \\ &\quad \begin{pmatrix} l_i & l_j & \lambda \\ m_i & -m_j & m_j - m_i \end{pmatrix}^2 [\mathcal{R}_{ij}^\lambda(k)]^2. \end{aligned} \quad (45)$$

Considering again the *non-averaged* incoherent scattering function in the special case of completely filled sub-shell  $l_i, l_j$ , the summations over  $m_i$  and  $m_j$  remove the angular dependence on  $\hat{k}$ . The filled sub-shells thus contribute

$$2(2l_i + 1)(2l_j + 1) \sum_{\lambda} (2\lambda + 1) \begin{pmatrix} l_i & l_j & \lambda \\ 0 & 0 & 0 \end{pmatrix}^2 [\mathcal{R}_{ij}^\lambda(k)]^2$$

to the incoherent form factor, with a factor 2 for the spin multiplicities in both sub-shells (rather than a factor 4, because the cross terms between sub-shells with opposite spin projections drop out due to the orthogonality of the spin orbitals).

Except for  $Z = 58$  (Ce, not of interest to us) all atoms with  $Z \leq 90$  have in their ground state only one sub-shell that is neither half nor completely filled [19]. (In atoms with two open sub-shells, one of them has  $l = 0$ .) Thus we need not consider the  $m$ -averaging procedure for cases where  $m_i$  and  $m_j$  come from two different partially filled sub-shells with  $l_i > 0$  and  $l_j > 0$ . In the cases of our interest averaging over  $m_i$  and  $m_j$  is then straightforward. The  $m$ -averaged contribution from two different sub-shells reads

$$\frac{1}{2} \nu_i \nu_j \sum_{\lambda} (2\lambda + 1) \begin{pmatrix} l_i & l_j & \lambda \\ 0 & 0 & 0 \end{pmatrix}^2 [\mathcal{R}_{ij}^\lambda(k)]^2$$

where  $\nu_i$  and  $\nu_j$  denote the occupation numbers of the two sub-shells and the factor 1/2 stems from the orthogonality of spin orbitals. If  $i$  and  $j$  both refer to the same sub-shell the multiplicity factor is slightly more complicated, depending on whether the sub-shell is less than, or more than, half filled. For this limited number of cases, we again determined the  $m$ -dependent part by suitably averaging over all possible distributions of  $m$  values in a partially filled sub-shell.

## 5. Some other models

For comparison we briefly discuss in this section some simple alternative models for evaluating the coherent and incoherent form factors,  $F_{00}(k)$  and  $S_{\text{inc}}(k)$ , respectively, for application in complex atomic scattering. Specifically, we will use analytical screening models [20, 21] to derive the elastic form factors. The inelastic scattering functions can then be obtained from the elastic form factors either in the no-correlation limit, or from an argument due to Heisenberg and based on the Thomas-Fermi model.

The simplest possible model to describe the effect of incoherent scattering off the atom's electrons would merely divide the cross section for coherent scattering (scaling with  $Z^2$ ) by  $Z$ , on the grounds that everything remains the same except that each electron contributes incoherently to the cross section (complete "anti-screening"). We found that this approach underestimates the incoherent scattering cross section by as much as 50%. For typical targets like Ti or Ni this implies an error of roughly 2% in the target-inclusive cross section, clearly beyond the required limit of 1%.

### 5.1. Elastic form factors

In order to simplify the atomic structure calculation, one might use the Thomas-Fermi model to replace the density  $\rho(\mathbf{r})$  occurring in

$$F_{00}(\mathbf{k}) = \int d^3r \rho(\mathbf{r}) \exp(i\mathbf{k} \cdot \mathbf{r}). \quad (46)$$

Expressing the potential due to the charge distribution of the electrons in the form

$$V(r) = -\frac{Z}{r}\chi(r), \quad (47)$$

the corresponding charge distribution is given by the second derivative of the screening function:

$$\rho(r) = \frac{Z}{4\pi r} \chi''(r). \quad (48)$$

Here and in the following the prime denotes differentiation with respect to  $r$ . For a spherical charge distribution the coherent form factor reduces to the monopole term. Using Molière's [21] parameterization for  $\chi$ ,

$$\chi(r) = \sum_{i=1}^3 B_i \exp(-\beta_i r/b); \quad (49)$$

$$B_1 = 0.1; B_2 = 0.55; B_3 = 0.35; \quad (50)$$

$$\beta_1 = 6.0; \beta_2 = 1.2; \beta_3 = 0.3; \quad (51)$$

with  $b = a_{\text{Bohr}}(9\pi^2/128)^{1/3} Z^{-1/3}$ , the coherent form factor reads

$$F_{00}(k) = Z \sum_{i=1}^3 B_i \frac{1}{1 + (b k/\beta_i)^2}. \quad (52)$$

for the electronic part, and again  $F_{\text{Atom}}(k) = Z - F_{00}(k)$ . The same analytical form with different parameters  $B_i$  and  $\beta_i$  determined by fitting expectation values of powers of  $r$  to exact Dirac-Hartree-Fock-Slater results is used in [20] where the fitting parameters for all  $Z \leq 92$  may be found as well.

### 5.2. Inelastic form factors: No-correlation limit

Inserting the elastic form factor of the previous subsection into (42) we are left with the evaluation of

$$\sum_{i=1}^Z \sum_{j \neq i} \langle \Psi_0 | \exp(i\mathbf{k} \cdot [\mathbf{r}_j - \mathbf{r}_i]) | \Psi_0 \rangle = Z(Z-1) \int d^3r d^3r' N_2(\mathbf{r}, \mathbf{r}') \exp(i\mathbf{k} \cdot [\mathbf{r} - \mathbf{r}']) \quad (53)$$

where we have already integrated over all variables not pertaining to the orbitals  $i$  and  $j$ . Here the function  $N_2(\mathbf{r}, \mathbf{r}')$  describes the probability of finding any two of the properly anti-symmetrized electrons at positions  $\mathbf{r}$  and  $\mathbf{r}'$ . The *no-correlation limit* now replaces this two-particle density by the product of the single-particle probabilities  $\rho(\mathbf{r})/Z$  and  $\rho(\mathbf{r}')/Z$ . The integral in the last expression then reduces to  $|F_{00}(\mathbf{k})/Z|^2$ , i.e., the square of the elastic form factor normalized per electron. As there are  $Z(Z-1)$  such terms in the double sum over  $i, j$ , we finally find

$$S_{\text{inc}}(\mathbf{k}) = Z - |F_{00}(\mathbf{k})|^2/Z. \quad (54)$$

Using the elastic form factor of the previous subsection, this result provides a simple expression for  $S_{\text{inc}}$ . However, we have made here the crucial assumption that there is no correlation between the electrons in different orbitals. In a single-particle picture this amounts to assuming that all single-particle states are available for all electrons simultaneously. Pauli blocking, i.e., the fact that due to the Pauli exclusion principle some states  $X$  cannot be excited for a given electron because they are occupied by other electrons, is then disregarded completely. Since in this limit the (incoherent) summation over  $X$  also includes the Pauli blocked states, the expression (54) clearly overestimates the correct scattering function.

### 5.3. Thomas-Fermi model for incoherent scattering

Following Heisenberg [22] we can find a simple expression for the *incoherent* atomic form factor, going beyond the no-correlation limit but remaining in the spirit of the Thomas-Fermi model (see also [23]). Expanding the squared modulus in the incoherent sum (43) we write

$$S_{\text{inc}}(\mathbf{k}) = Z - \int d^3r d^3r' \exp(i\mathbf{k} \cdot (\mathbf{r} - \mathbf{r}')) \left| \sum_{j=1}^Z \Phi_j^*(\mathbf{r}) \Phi_j(\mathbf{r}') \right|^2. \quad (55)$$

In the Thomas-Fermi model, the density is related to the volume of a sphere in momentum space,

$$\sum_{j=1}^Z |\Phi_j(\mathbf{r})|^2 = \frac{2}{(2\pi)^3} \int_{\kappa \leq k_F(\mathbf{r})} d^3\kappa = \frac{1}{3\pi^2} [2|V(\mathbf{r})|]^{3/2}. \quad (56)$$

Heisenberg generalized this expression to obtain the two-particle density as an integral in momentum space (with  $\mathbf{r}_1 = (\mathbf{r} + \mathbf{r}')/2$ )

$$\sum_{j=1}^Z \Phi_j^*(\mathbf{r}) \Phi_j(\mathbf{r}') = \frac{2}{(2\pi)^3} \int_{\kappa \leq k_F(\mathbf{r}_1)} d^3\kappa \exp(i\mathbf{k} \cdot (\mathbf{r} - \mathbf{r}')) \quad (57)$$

which reduces to the Thomas-Fermi expression for  $\mathbf{r} = \mathbf{r}'$ . (55) now contains additional six-fold integration over  $d^3\kappa$  and  $d^3\kappa'$ . Performing these integrations as well as the integration over  $(\mathbf{r} - \mathbf{r}')$ , we find (following Heisenberg's argument about the

common volume of two intersecting spheres in momentum space, and paying attention to the spin multiplicity)

$$S_{\text{inc}}(\mathbf{k}) = Z - \frac{4}{3\pi} \int_0^{r_0} dr_1 r_1^2 (\sqrt{2V(r_1)} - k/2)^2 (\sqrt{2V(r_1)} + k/4), \quad (58)$$

where the integration over  $\mathbf{r}_1$  is restricted to the region of coordinate space with  $k_{\text{F}}(\mathbf{r}_1) \geq k/2$  since otherwise the two spheres in momentum space do not overlap.

Using  $V(r) = (Z/r)\chi(r)$  the incoherent form factor turns into

$$S_{\text{inc}}(k) = Z - \frac{4}{3\pi} \int_0^{r_0} dr \sqrt{r} [2Z\chi(r)]^{3/2} + \frac{2}{\pi} Z k \int_0^{r_0} dr r \chi(r) - \frac{1}{36\pi} (k r_0)^3 \quad (59)$$

where the upper limit of integration  $r_0$  must satisfy

$$\frac{Z}{r_0} \chi(r_0) = \frac{1}{8} k^2. \quad (60)$$

Within the frame work of the Thomas-Fermi model, the screening function satisfies the differential equation

$$\frac{Z}{r} \frac{d^2}{dr^2} \chi(r) = \frac{4}{3\pi} [(2Z/r)\chi(r)]^{3/2}; \quad \chi(0) = 1, \quad (61)$$

thus enabling us to replace the first integral in (59). The second derivative of  $\chi$  can then be removed by integrating by parts, yielding

$$S_{\text{inc}}(k) = -Z r_0 \chi'(r_0) + \frac{2}{\pi} Z k \int_0^{r_0} dr r \chi(r) + \frac{1}{8} r_0 k^2 - \frac{1}{36\pi} (k r_0)^3. \quad (62)$$

From (59) and (62) we note that this simple model does not reproduce the correct limit as  $k \rightarrow 0$ : In this limit  $r_0 \rightarrow \infty$ , and the integral in (62) assumes a constant non-zero value. Thus  $S_{\text{inc}}$  grows *linearly* with  $k$ . By contrast the expression in the no-correlation limit (containing  $F_{00}(k)$ ) grows with  $k^2$ , as does the Hartree-Fock-Slater result derived in the preceding section (since the term linear in  $k$  drops out of the expansion in (42) due to the symmetry under interchange  $i \leftrightarrow j$ ).

## 6. Numerical method and results

In our application to scattering of pionium on atomic targets, we use hydrogenic wavefunctions for the pionium system  $\pi^+\pi^-$ . The corresponding form factors  $F_{00,\Pi}$  and  $S_{\text{inc},\Pi}$  are evaluated analytically as described in [7].

Section 4 provides expressions for the evaluation of coherent atomic form factors and incoherent scattering functions in the framework of the Dirac-Hartree-Fock-Slater formalism. In our calculations we start from a simple analytical charge distribution for the electrons as given e.g. in [20] or similarly in [21]. Taking the electronic structure of the elements from [19] we solve either the Schrödinger or the Dirac radial equation for each occupied orbital, treating exchange effects by Latter's approximation (see e.g. [20]). The resulting charge density is then used to obtain improved radial orbitals, iterating the process until self-consistency is reached. Even for heavy elements with electrons in some twenty different orbitals and requiring several ten iterations, this calculation is readily performed with the help of the program package RADIAL [24].

Using these orbitals we evaluate the radial integrals in (39) and (45) on a reasonably dense mesh of  $k$  values with the help of an integration routine developed for integrals containing spherical Bessel functions and powers [25]. To this end, the numerical solutions for the orbitals obtained on a grid of  $r$  values are replaced by

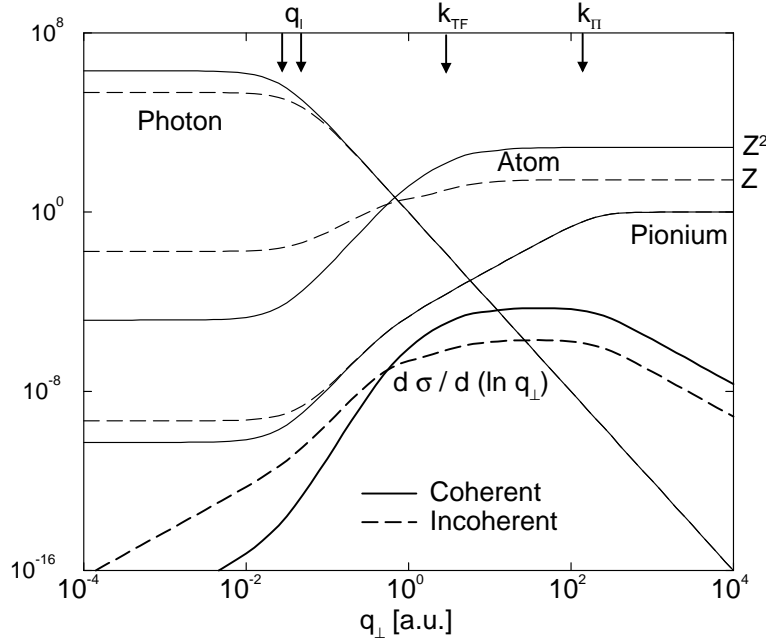


**Figure 2.** Various contributions to the integrand for the cross section vs.  $q_{\perp}$ , on a log-log scale. To compensate for the logarithmic  $q_{\perp}$ -axis, the integrand is represented as  $d\sigma/d \ln q_{\perp}$ . The individual curves are labelled in the figure. The cross sections correspond to target-elastic (solid lines) and target-inelastic (dashed lines) pionium scattering off Ni ( $Z = 28$ ) at a projectile energy  $E = 5$  GeV, summed over all final states of the pionium. The arrows at the upper edge indicate the relevant momentum scales. See text for details.

piecewise splines. The angular parts for the partially filled sub-shells are determined by averaging over all distributions of magnetic quantum numbers  $m$  in accordance with the Pauli principle, as described in section 4.

Let us first investigate the range of  $q_{\perp}$  relevant for the cross section as given by (9) or (18). Figure 2 demonstrates the interplay of different momentum scales associated with the photon, with the atom, and with the pionium, respectively. The figure shows the integrand from (9) in singly differential form:

$$\frac{d\sigma}{dq_{\perp}} = 2\pi q_{\perp} \frac{4\alpha^2}{\beta^2} (\text{Photon}) \times (\text{Atom}) \times (\text{Pionium}), \quad (63)$$

together with its decomposition into photon, atom and pionium parts (cf. (8)):

$$(\text{Photon}) = \frac{1}{q^4} = \frac{1}{(q_{\parallel}^2 + q_{\perp}^2)^2}, \quad (64)$$

$$(\text{Atom}) = W_{2,A} = \begin{cases} |F_{00,A}(q)|^2 & \text{for coherent scattering,} \\ (q^4/k^4) S_{\text{inc},A}(k) & \text{for incoherent scattering,} \end{cases} \quad (65)$$

$$(\text{Pionium}) = W_{2,\Pi} = (q^4/s^4) S_{\text{inc},\Pi}(s). \quad (66)$$

The solid lines refer to the total cross section (i.e., summed over all pionium final states) for target-elastic scattering off Ni ( $Z = 28$ ) for pionium in its ground state. The projectile energy is 5 GeV. The dashed lines correspond to the same setting for

the target-inelastic process. Here the integrations over  $\omega$  and  $\Delta$  in (9) have been replaced by setting an average excitation energy for the ponium at  $\omega_0 = 1.858$  keV (ground state binding energy), and for the atom we set  $\Delta_0 = 0$  (target-elastic) and  $\Delta_0 = 100$  eV (target-inelastic), respectively.

The arrows indicate the relevant momentum scales:  $q_l$  for the photon,  $k_{\text{TF}} = Z^{1/3}/a_{\text{Bohr}}$  for the atom, and  $k_{\Pi}$  for the ponium. The arrow on the left under the label “ $q_l$ ” corresponds to target-elastic scattering, while the one on the right corresponds to incoherent scattering (with non-zero  $\Delta_0$  and thus with a larger  $q_l$ ). For  $q_{\perp} \ll q_l$ , the photon momentum is essentially given by the constant  $q_l$ . When  $q_{\perp} \gg q_l$ , on the other hand, this part displays a  $1/q_{\perp}^4$  behavior. The atomic part shows an increase between  $q_l$  and several inverse Bohr radii (indicated by  $k_{\text{TF}}$ ). As expected,  $|F_{00,A}(k)|^2$  grows roughly with  $q_{\perp}^4$ , whereas  $S_{\text{inc},A}(k)$  grows only with  $q_{\perp}^2$ . At  $q_{\perp} \approx 5k_{\text{TF}}$  the atomic part reaches its asymptotic value ( $Z^2$  or  $Z$ , respectively). In this regime the ponium part only just starts to contribute appreciably. It grows quadratically with  $q_{\perp}$  to saturate at a few multiples of the ponium scale  $k_{\Pi}$ . The product of the three factors clearly demonstrates that the main contributions to the cross sections come from the range of  $q_{\perp}$  between  $k_{\text{TF}}$  and  $k_{\Pi}$ .

In figure 2 we set  $\omega_0 = E_{\text{bind},\Pi}$  for the ponium, as well as a non-zero value for  $\Delta_0$  in the case of incoherent scattering. The specific choice for these average excitation energies is guided by the following observations. For coherent (target-elastic) scattering  $\Delta_0 \equiv 0$ , and any ambiguity in calculating total cross sections from (18) is limited to the choice of an appropriate  $\omega_0$ . From a comparison [7] of total cross sections for coherent scattering in the closure approximation with the “exact” total cross sections obtained by accumulating partial cross sections for bound-bound and bound-free ponium transitions (summation/integration over all final states), we note that bound-bound transitions (excitation and de-excitation) account for the major part of the total cross section. Typically, breakup (ionization) accounts for some 30%–40% of the total cross section in the ground state, decreasing roughly by a factor  $n^2$  for ponium in the initial state  $(n, l)$ . Furthermore, most of the breakup cross section from a given initial state comes from the range of continuum energies from 0 to about  $E_{\text{bind},\Pi}$  above the continuum threshold. Therefore the average energy difference between initial and all final states—weighted by their contribution to the total cross section—is of the order of the binding energy  $E_{\text{bind},\Pi}$ .

Figure 3a) shows the total cross section for elastic scattering in the closure approximation as a function of  $\omega_0$  (in units of  $E_{\text{bind},\Pi}$ ). The total cross sections have been normalized to their values at  $\omega_0 = 0$ . As can be seen from the figure, only the ground state total cross section varies appreciably over a reasonable range of  $\omega_0$  values. We also find [7] that the closure cross sections at  $\omega_0 = E_{\text{bind},\Pi}$  coincide with the converged accumulated partial cross sections. We therefore set  $\omega_0 = E_{\text{bind},\Pi}$  in the following.

In frame b) of the same figure we show the dependence on the average atomic excitation energy  $\Delta_0$  for the target-inelastic scattering process. Here the ponium energy has been fixed at  $\omega_0 \approx 1.858$  keV. Since we calculate  $S_{\text{inc}}(k)$  using individual orbitals, we can easily determine the contributions resolved with respect to atomic shells, or even per individual electron as in figure 3b). The tabulated values for the atomic incoherent scattering functions [16] cannot serve to study the closure approximation’s sensitivity to the atomic excitation energy. When varying  $\Delta_0$  from 0 to several keV, it is important to distinguish whether this excitation energy is transferred to an electron in the  $K$  shell or to one of the outer electrons. In the latter



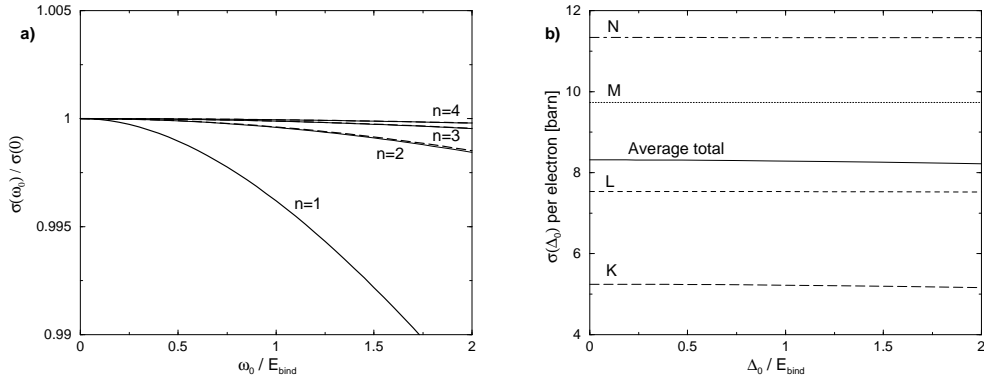


**Figure 3.** **a)** Closure cross sections (normalized to  $\omega_0 = 0$ ) versus  $\omega_0$  (in units of  $E_{\text{bind},\Pi}$ ) for *coherent* scattering of pionium in various initial states as indicated in the figure. Target material is Ni, projectile energy is 5 GeV. Solid lines: initial  $s$  states; dashed lines: initial  $p$  states of the pionium. **b)** Contributions of individual target electrons to the closure cross section for *incoherent* scattering of pionium in its ground state, plotted versus average atomic excitation energy  $\Delta_0$  (normalized to the average binding energy of the respective atomic shells, ranging from some 10 eV for the  $N$ -shell to  $\sim 5$  keV for the  $K$ -electrons). Also shown is the average contribution of all shells (total incoherent cross section divided by  $Z$ ). Target material is Ti, projectile energy is 5 GeV.

case, the atomic electron is excited into a high energy continuum state. This process contributes very little to the incoherent cross section which—like the pionium’s cross section—is dominated by excitation rather than by ionization. The average excitation energy  $\Delta_0$  for each curve in figure 3b) has been normalized to the binding energy of the individual shells (averaged over sub-shells). We note that the individual contributions are roughly proportional to the principal quantum number of each electron. Combined with the fact that the outer shells typically accommodate many more electrons than the inner shells, we find that the target-inelastic (incoherent) scattering process is clearly dominated by the loosely bound outer electrons. At the same time figure 3b) also demonstrates that the incoherent scattering cross section is almost independent of  $\Delta_0$ . Thus we may safely set  $\Delta_0 = 0$  in our calculation.

As a verification and further illustration of these findings, figure 4 displays  $d\sigma_{\text{inc}}/d\ln q_{\perp}$  for ground state pionium scattering incoherently off Ti ( $Z = 22$ ) at 5 GeV projectile energy. The solid line corresponds to the integrand for incoherent scattering (18) calculated using (45). In these calculations we set  $\omega_0 = 1.858$  keV, the binding energy of the pionium, and  $\Delta_0 = 0$ . As can be seen from the dashed line in the figure, the simplest approximation consisting of scaling the target-elastic (coherent) cross section by  $1/Z$  clearly underestimates the correct result. At the same time the dash-dotted (chain) curve shows that the approximation using the coherent form factor (39) in the no-correlation limit obviously overestimates the correct result by an even larger amount. In more detail we find that the ratio  $(\sigma_{\text{coh}}/Z) : \sigma_{\text{inc}}$  for pionium initially in the ground state amounts to 0.49 (!) for a Li target, 0.62 (Al), 0.66 (Ti), 0.73 (Ni), 0.72 (Mo), and 0.74 (Pt). For pionium initially in  $2s$  or  $3s$  states, these ratios range from 0.65 (Li) to 0.80 (Pt) for these targets relevant in the experiment. For the lighter targets, these huge uncertainties of the incoherent part

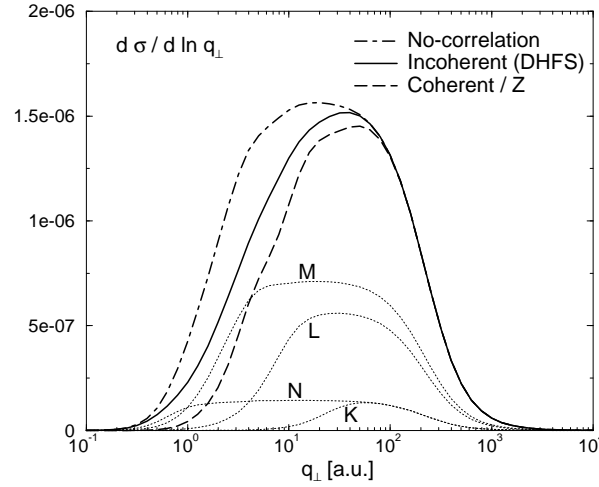


**Figure 4.** Integrand for incoherent (target-inelastic) cross section of ground state pionic scattering off Ti at energy 5 GeV, versus  $q_{\perp}$  (on a log-scale). The areas under the curves yield the respective cross sections. Calculations with  $\omega_0 = 1.858$  keV and  $\Delta_0 = 0$ . The contributions from the individual shells (dotted lines) are labelled in the figure.

result in considerable errors in the inclusive cross sections: The ratio

$$\frac{\sigma_{\text{coh}}(1 + 1/Z)}{\sigma_{\text{coh}} + \sigma_{\text{inc}}}$$

amounts to 0.795 (Li), 0.958 (Al), 0.978 (Ti), 0.987 (Ni), 0.991 (Mo), and 0.996 (Pt). Thus only for the heavy targets the required accuracy of 1% can be attained with such a crude approximation for the incoherent part.

Further in figure 4, the dotted lines show the contributions to the incoherent scattering cross section resolved according to atomic shells. A direct comparison of the areas enclosed between the individual lines and the abscissa demonstrates that the ten  $M$ -electrons dominate the cross sections, followed by the eight  $L$ -electrons. Also, the two  $N$ -electrons contribute considerably more strongly than the  $K$ -electrons, whose influence is limited to rather large  $q_{\perp}$  as expected.

Figures 2 and 4 show clearly that the principal contributions to the cross sections come from the region  $k_{\text{TF}} < q_{\perp} < k_{\text{II}}$ . Thus the long-wavelength limit applies for the pionic (but not for the atom). Furthermore we noted that the relevant excitation energy  $\Delta_0$  is small and may safely be set to zero, and thus  $W_{1,A} = 0$ . Under these circumstances the cross section due to the transverse part of the current operator is given by (31) and (33). In figure 5 we show the ratio between the cross sections for the transverse electric part ( $T^e$ ) and the one for the Coulomb part ( $M^C$ ), as a function of the average pionic excitation energy  $\omega_0$ . Note that the ratio is given in per cent. The solid lines correspond to total cross sections for coherent scattering of pionic in various initial  $s$ -states as indicated in the figure. The dashed lines correspond to the target-inclusive process (with  $\Delta_0 = 0$ ). At the typical average pionic excitation energy  $\omega_0 = E_{\text{bind}}$  the transverse cross section  $\sigma^T$  for coherent scattering amounts to 0.4% of the Coulomb part in the ground state, decreasing rapidly for initially excited states of the pionic.

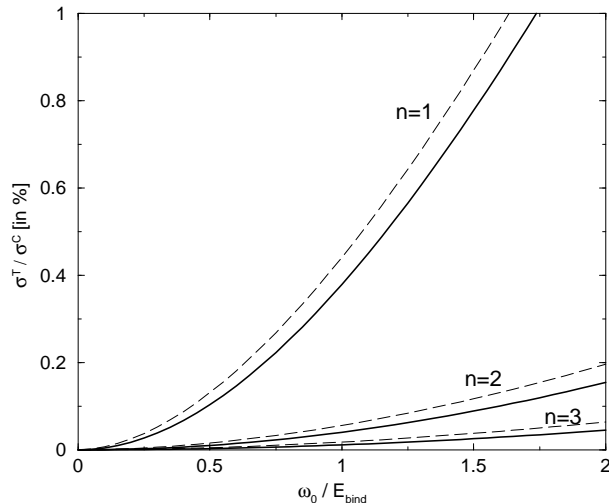


**Figure 5.** Ratio (in per cent) between transverse electric and Coulomb contributions to the total cross section of pionium scattering off Ni at 5 GeV, as a function of  $\omega_0$ . Solid line: target-elastic process; dashed line: target-inclusive process. Pionium initial states (with  $l_i = 0$ ) are indicated in the figure.

Finally figure 6 compares various models for  $F_{00,A}$  and  $S_{\text{inc},A}$  over the range of  $k$  values relevant for our calculations of cross sections in the context of experiment DIRAC. The solid lines correspond to our calculations using (39) for the coherent form factor and (45) for the incoherent scattering function, respectively. We use relativistic Dirac orbitals in both cases. The squares represent tabulated values from two compilations of state-of-the-art Hartree-Fock calculations with various corrections (configuration interaction, relativistic effects, a.s.o.). Note that while the tabulated results for  $F_{00}$  correspond to relativistic calculations [26], the tables for  $S_{\text{inc}}$  in [16] contain only non-relativistic results. The log-log representation in the left frame serves merely to display the asymptotic behavior of the simple models discussed in section 5. Analyzing the dashed line corresponding to (52) we note that the incorrect asymptotic fall-off for  $F_{00}$  at large  $k$  poses no difficulties. In the right panel we see that between  $5 \leq k \leq 10$  a.u. the Thomas-Fermi-Molière model misses features of the atomic shell structure, but the resulting deviation from (39) is insignificant. Much more problematic are the crude approximations for  $S_{\text{inc}}$ . While the no-correlation limit (54), using (52) and shown with the dotted line, increases with  $k^2$  at small  $k$  (as it should), it dramatically overestimates the scattering function in the most relevant range between 0.1 and 100 a.u. On the other hand, the Thomas-Fermi model for incoherent scattering as developed by Heisenberg [22], with modifications [23, App. B] for the use of Molière’s approximation, is quite successful at  $k \geq 5$  a.u., but it fails completely at smaller  $k$ .

## 7. Conclusions

We have reviewed the formalism for incoherent atomic scattering. The basic expressions for the atomic form factors and scattering functions have then been evaluated in the framework of Dirac-Hartree-Fock-Slater theory, i.e., using numerically

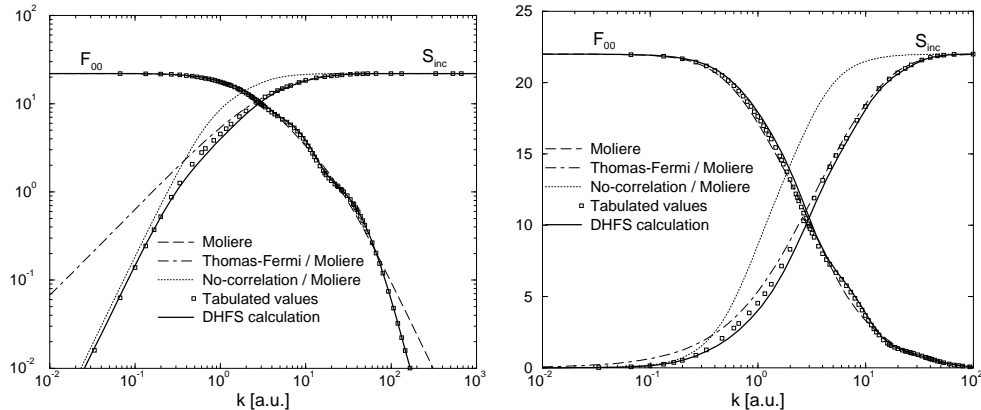


**Figure 6.** Electronic part  $F_{00}$  of the coherent atomic form factor and incoherent scattering function  $S_{\text{inc}}$  for Ti ( $Z = 22$ ). The asymptotic behavior is more easily seen from the log-log diagram on the left. The range of relevance for the cross section calculations is  $0.1 \leq k \leq 100$  a.u. For an explanation of the different models, see text.

determined electron orbitals. For comparison, both the form factor for coherent scattering, as well as the incoherent scattering function have been derived in simple analytical models based on the Thomas-Fermi model of the atom. Applying these different descriptions we performed detailed numerical studies in the context of pionium scattering incoherently off the electrons of various target atoms. Due to the much larger reduced mass of the pionium system ( $\mu_{\Pi} = m_{\pi}/2 \approx 136.566m_e$ ), the length and momentum scales of the pionium and the target atom are very different.

An investigation of the relevant momentum transfer  $q_{\perp}$  revealed that the cross sections are dominated by the contributions from the region between the Thomas-Fermi momentum  $k_{\text{TF}} = Z^{1/3}/a_{\text{Bohr}}$  for the atom, and the momentum scale of the pionium at  $k_{\Pi} = \mu_{\Pi}/a_{\text{Bohr}}$ . Under these circumstances the simple models for incoherent scattering discussed in section 5 prove not sufficiently accurate for our application in the context of pionium-atom scattering with a required accuracy of 1% or better. Whereas the analytical models discussed in section 5 provide sufficiently accurate *coherent* form factors, the *incoherent* contribution really requires the more accurate treatment developed in section 4, despite its lesser importance (as compared to coherent scattering). Only an explicit DHFS calculation can provide satisfactory scattering functions. Since the target materials employed in experiment DIRAC will be as heavy as Pt, our calculation with relativistic orbitals is clearly more appropriate than the non-relativistic results tabulated in [16].

From our detailed discussion of the  $q_{\perp}$ -dependence of the integrand for the cross section we also conclude that the loosely bound outer shell electrons dominate the target-inelastic cross sections. Their contribution to the integrand  $d\sigma/dq_{\perp}$  covers a much larger range of  $q_{\perp}$  values than the one corresponding to inner shell electrons. Following this argument further, free electrons would show a behavior rather similar to the one of the outer shells, their contribution to the cross section would stretch even further down to smaller  $q_{\perp}$ . However, the cross section hardly depends on this modification at very small  $q_{\perp}$ . Our calculation therefore applies equally well to quasi-free electrons and to electrons in the conduction band. Thus solid state effects and

chemistry need not be considered explicitly as they prove irrelevant for calculations pertaining to experiment DIRAC. The same conclusion had been inferred in our earlier study [7] based on an analysis of the relevant impact parameter range. Recalling that target-inelastic scattering constitutes merely a correction of order  $1/Z$  of the atomic part, variations on the order of a few per cent in the incoherent scattering cross sections are insignificant.

These findings are confirmed in our analysis of the dependence of the cross sections on the average excitation energies for ponium and atom. Our calculation of incoherent scattering contributions resolved according to individual target electron shells demonstrates that the average excitation energy for the atom may safely be set to zero,  $\Delta_0 = 0$ . This information which is crucial for the closure approximation cannot be extracted from the scattering functions in [16]. For the ponium, on the other hand, a non-vanishing excitation energy in the amount of the binding energy is needed when calculating total cross sections in the closure approximation in order to get agreement between the closure result and the result obtained by explicitly summing the partial cross sections over all final states.

Earlier investigations on ponium-atom interaction [11, 7] invoked properties of the hydrogen-like ponium system to obtain crude estimates for the magnitude of the magnetic terms so far neglected in this interaction. From the non-relativistic wavefunctions for the ponium, its internal velocity is of the order of  $v/c \approx \alpha/2$ . Thus magnetic terms are believed to be small of this order. We established a much better justified estimate for the magnetic terms (actually for the transverse part of the current) in the long-wavelength limit. Our investigation showed that this limit applies very well for the ponium, whereas it does not apply for the atom. However, the transverse current does not contribute in the elastic case on the atom side, and for the inelastic case it is suppressed even more than the corresponding term on the ponium side because the relevant atomic excitation energies (of the outer shells) are smaller than those of the ponium.

## Acknowledgments

We would like to thank R.D. Viollier, J. Schacher, L. Nemenov, and L. Afanasyev for stimulating discussions on the subject of this article. Special thanks are due to Zlatko Halabuka whose efficient and accurate integration routine proved instrumental in the calculation of atomic form factors and scattering functions. We also wish to thank an unknown referee for fruitful and stimulating comments.

## References

- [1] McGuire J H, Stolterfoht N and Simony P R 1981 *Phys. Rev. A* **24** 97
- [2] Anholt R 1985 *Phys. Rev. A* **31** 3579
- [3] Wheeler J A and Lamb W E Jr 1939 *Phys. Rev.* **55** 858
- [4] Sørensen A H 1998 *Phys. Rev. A* **58** 2895
- [5] Voitkiv A B, Grün N and Scheid W 1999 *Phys. Lett. A* **260** 240
- [6] Adeva B *et al* 1995 *Lifetime measurement of  $\pi^+\pi^-$ -atoms to test low-energy QCD predictions* CERN/SPSLC 95-1, SPSLC/P 284; see also <http://www.cern.ch/DIRAC/>.
- [7] Halabuka Z, Heim T A, Hencken K, Trautmann D and Viollier R D 1999 *Nucl. Phys.* **B554** 86
- [8] de Forest T and Walecka J D 1966 *Adv. Phys.* **15** 1
- [9] Halzen F and Martin A D 1984 *Quarks and Leptons* (New York: John Wiley)
- [10] Greiner W and Schäfer A 1995 *Quantum Chromodynamics* (Berlin: Springer)
- [11] Afanasyev L G *et al* 1994 *Phys. Lett.* **B338** 478

- [12] Voitkiv A B, Gail M and Grün N 2000 *J. Phys. B: At. Mol. Opt. Phys.* **33** 1299; Voitkiv A B, Grün N and Scheid W 2000 *Phys. Rev. A* **61** 052704
- [13] Walecka J D 1983 *ANL-83-50* (Argonne National Laboratory; unpublished)
- [14] Hencken K, Trautmann D and Baur G 1995 *Z. Phys. C* **68** 473
- [15] Blatt J M and Weisskopf V F 1952 *Theoretical Nuclear Physics* (New York: John Wiley)
- [16] Hubbell J H, Veigele Wm J, Briggs E A, Brown R T, Cromer D T and Howerton R J 1975 *J. Phys. Chem. Ref. Data* **4** 471
- [17] Slater J C 1960 *Quantum theory of atomic structure* (New York: McGraw-Hill) Chapters 13ff
- [18] Baur G, Hencken K and Trautmann D 1998 *J. Phys. G: Nucl. Part. Phys.* **24** 1657
- [19] Caso C *et al* (Particle Data Group) 1998 *Eur. Phys. J. C* **3** 1
- [20] Salvat F, Martínez J D, Mayol R and Parellada J 1987 *Phys. Rev. A* **36** 467
- [21] Molière G 1947 *Z. Naturforsch.* **2a** 133
- [22] Heisenberg W 1931 *Phys. Zeitschr.* **32** 737
- [23] Tsai Y S 1974 *Rev. Mod. Phys.* **46** 815
- [24] Salvat F, Fernández-Varea J M and Williamson W Jr 1995 *Comput. Phys. Commun.* **90** 151
- [25] Halabuka Z, private communication
- [26] Hubbell J H and Øverbø I 1979 *J. Phys. Chem. Ref. Data* **8** 69